Simultaneous optical tuning of hole and electron transport in ambipolar WSe_2 interfaced with a bicomponent photochromic layer: From high-mobility transistors to flexible multilevel memories

Haixin Qiu, Zhaoyang Liu, Yifan Yao, Martin Herder, Stefan Hecht, Paolo Samorì[*]

H. Qiu, Dr. Z. Liu, Dr. Y. Yao, Prof. P. Samorì

University of Strasbourg, CNRS, ISIS UMR 7006, 8 Alleé Gaspard Monge, F-67000 Strasbourg, France.

Email: samori@unistra.fr

Dr. M. Herder, Prof. S. Hecht

Department of Chemistry and IRIS Adlershof, Humboldt-Universität zu Berlin, 12489, Berlin, Germany.

Prof. S. Hecht

DWI - Leibniz Institute for Interactive Materials, Forckenbeckstr. 50, 52056 Aachen, Germany, & Institute of Technical and Macromolecular Chemistry, RWTH Aachen University, Worringer Weg 2, 52074 Aachen, Germany.

Keywords: ambipolar two-dimensional semiconductors, photochromic molecular blend, energy-level phototuning, multilevel memories, flexible electronics

Abstract: The interfacing of two-dimensional materials (2DMs) with photochromic molecules provides an efficient solution to reversibly modulate their outstanding electronic properties and offers a versatile platform for the development of multifunctional field-effect transistors (FETs). Herein optically switchable multilevel high-mobility FETs based on few-layer ambipolar WSe_2 are realized by applying on its surface a suitably designed bicomponent diarylethene (DAE) blend, in which both, hole and electron transport can be *simultaneously* modulated for over 20 cycles. The high output current modulation efficiency (97% for holes and 52% for electrons) ensures 128 distinct current levels, corresponding to a data storage capacity of 7 bit. The device is also implemented on a flexible and transparent polyethylene terephthalate substrate, rendering the 2DMs/DAEs hybrid structures promising candidates for flexible multilevel nonvolatile memories.

Atomically thin two-dimensional materials (2DMs) combining exceptional electronic, optical, and mechanical properties, as well as chemical stability, are promising candidates as key components for various applications spanning from (opto)electronics,[1-3] photonics,[4] sensing,[5, 6] to ultra-flexible and wearable electronics,[7-9] in the post-silicon era. In the past decade the scientific community has witnessed the booming of fundamental studies as well as technological advancements in the field of 2DMs. Alongside exploring their intrinsic properties, various physical and chemical modification strategies have been adopted in order to tune the 2DM's functions and device performances.[10, 11] Among them, achieving a tunable control over the electronic properties of 2DMs without introducing any defects still remains a major challenge,[12, 13] which is at the same time highly appealing for the development of practical multilevel stimuli-responsive electronics.[14-16] The interfacing with molecular systems possessing tunable structures and functionalities constitutes an efficient and versatile approach to provide different charge carrier doping levels and thus to reversibly modulate the opto-electronic properties of 2DMs.[17, 18] For example, it has been demonstrated that photochromic molecules, capable of undergoing reversible isomerization between two different states induced by light stimuli,[19] can serve as optically-responsive components when employed to functionalize unipolar 2DMs.[20, 21] Importantly, such hybrid structures take full advantage of the ultra-high sensitivity of 2DMs to any subtle environmental change,[18] which will emerge as an additional molecular-driven photoresponsivity. This enables the 2DMs/photochromic molecules hybrid structures to serve as active components in superior multifunctional transistors/memories that can optically be addressed and operated due to efficient and highly sensitive ON/OFF switching upon irradiation with light at defined wavelengths.[22-25] We have recently demonstrated the unipolar modulation of either electron transport in few-layer WSe_2 or hole transport in few-layer black phosphorous-based optically switchable field-effect transistors (FETs) by interfacing suitable photochromic molecules as optical switching elements.[26] However, the *simultaneous* photo-modulation of both electron and hole transport

in the target 2D materials has not been achieved before. It would be of utmost importance for a practical multilevel transistor as well as for the development of responsive organic complementary circuits (CMOS like) and photo-tunable inverters. As a consequence the applicability of such 2DMs/photochromic molecules hybrid systems could largely be extended.

In our previous work, we focused on WSe_2 flakes possessing an n-type dominant ambipolar behavior, with its electron current (10^{-5} A) three orders of magnitude larger than the hole current (10^{-8} A). Therefore, the modulation of hole current by operation of the photochromic molecule was not visually distinguishable. Inspired by the phenomenon that the main type of charge carrier in WSe_2 changes with its thickness, ranging from p-type, ambipolar to n-type,[27] in this work we tackle *full ambipolar* switching of charge transport in 2DM/photochromic molecule blends. For this purpose, we target few-layer WSe_2 flakes with a more balanced ambipolar behavior, with its electron and hole current on the same scale (10^{-6} A). We propose an optically switchable multilevel FET by interfacing WSe_2 with a bicomponent DAE blend consisting of two DAE molecules with specific energy levels, which are engineered in order to be capable of trapping either the electrons or the holes of WSe_2. The device is demonstrated to be able to modulate both electron and hole transport *simultaneously* by remote light stimuli. The photo-modulation is demonstrated to be efficient and reversible with negligible switching fatigue after over 20 illumination cycles. Noteworthy, the output current modulation for holes is as high as 97%, while for electrons the modulation amounts to 52%. Moreover, such current modulation ratio can be readily tuned by controlling the light dose, which means by adjusting the irradiation duration the FET device can reach a multitude of current states. In particular, the balanced ambipolar characteristic of WSe_2 enables our device to attain 64 distinct current levels for both holes and electrons, as evidenced through a precise control and fine-tuning over the output current thereby highlighting its potential to be further developed into multilevel memories with data storage capacity of 7 bit.[28] Additionally, by taking advantage of the thermal bistability of DAE molecules in both photo-isomeric states,[29]

the device is shown to possess a prolonged retention time exceeding 20 days in the dark. This result outperforms the current state-of-the-art memories based on other photochromic molecules, such as spiropyrans and azobenzenes,[30, 31] and is highly promising for applications as non-volatile memories.[32] Remarkably, taking full advantage of the superior mechanical properties of ultra-thin 2D WSe_2, our device is also able to be operated on a flexible and transparent polyethylene terephthalate (PET) substrate, without losing its optical switching capability, which is attractive for future generation of multifunctional wearable electronics. When compared with memories based on organic semiconductors blended with DAE molecules,[33] our memories based on 2DMs show similar features while hold higher mobilities and miniaturizing size at the atomic level thickness.

The WSe_2 flakes are produced by mechanical exfoliation, which enables to preserve the outstanding electronic properties with an ambipolar transport behavior, suggesting the presence of both abundant free electron and hole charge carriers in the channel. The WSe_2 channel is further incorporated with a spin-coated blend film containing two DAE molecules possessing engineered energy levels, namely DAE_1[34] and DAE_2,[35] both of which feature tunable lowest unoccupied molecular orbital (LUMO)/highest occupied molecular orbital (HOMO) energy levels above or below conduction band (CB) and valence band (VB), respectively, of WSe_2.[36] Therefore, we are able to utilize the optically responsive nature of the photochromic molecules to modulate the charge transport of both electrons and holes in the WSe_2 channel. Figure 1a illustrates the detailed energy-level diagram of DAE_1, DAE_2, and WSe_2. The yellow bands represent the CB/VB of few-layer WSe_2. The electron transport modulation is realized by DAE_1, since the conduction band minimum (CBM) of WSe_2 (-3.5 eV) lies energetically between the LUMO levels of the open isomer (DAE_1o, -2.7 eV) and the closed isomer (DAE_1c, -3.7 eV). The lower LUMO of DAE_1c behaves as electron-accepting level (trapping the transferred electrons from WSe_2, thus reducing the current to gain modulation), while higher LUMO energy of DAE_1o impedes the electron transfer from WSe_2 (no

modulation). Similarly, the valence band maximum (VBM) of WSe_2 (-5.1 eV) is located between the HOMO of DAE_2o (-5.4 eV) and DAE_2c (-4.7 eV), enabling the modulation of hole transport. DAE_2c behaves as a trapping site (modulation) while DAE_2o only represents a scattering center for the holes (no modulation) travelling in WSe_2. In general, upon ultraviolet (UV) irradiation at 312 nm, both DAE molecules are converted to their closed photo-isomeric states, accompanied with a simultaneous transfer of electrons and holes from WSe_2 channel to DAEs, inducing a decrease of charge carrier density in the FET device as well as the current. Conversely, upon visible (vis) light irradiation at 530 nm the DAE molecules switch back to their open isomer states, resulting in full recovery of the charge carrier density within WSe_2 and the current. Note that in order to largely preserve the intrinsic electrical properties of WSe_2 and to minimize the perturbation of DAE molecules, the DAE blends are simply spin-coated onto the substrate in order to interact with WSe_2 flakes in a non-covalent fashion.

To assess the photo-switching ability of DAE molecules after physisorption on WSe_2, UV-vis absorption spectra of the DAE blend/WSe_2 film was initially recorded on quartz substrates. As displayed in Figure S1c, following UV irradiation, the intensity of the peak around 312 nm corresponding to open isomers clearly decreases, while another peak around 530 nm originating from the closed isomers appears. The original absorption features are recovered after vis irradiation. Therefore, the DAE molecules in the solid-state blended film are still able to undergo reversible photo-isomerization when physisorbed onto the surface of WSe_2. Importantly, both DAEs show similar molar absorptivities, speed of photoisomerization (quantum yields), and almost quantitative formation of the ring closed isomer under UV irradiation,[35] allowing for their fully simultaneous operation in the device.

Back-gated FETs with patterned top-contact Au electrodes onto Si/SiO_2 substrates were fabricated based on few-layer WSe_2 flakes by means of well-established photolithography (details provided in the Supporting information). Atomic force microscopy (AFM) topographical imaging of WSe_2 (Figure S2c) enabled to visualize the flakes and quantify their

thickness as ~4.3 nm. In order to explore the photo-modulation of the electrical properties of WSe_2, a DAE blend solution with mix weight ratio of 1:1 was spin-coated on top of the fabricated device. The surface roughness of WSe_2 flake was enhanced after molecular deposition with the average thickness increasing to ~6.9 nm, thereby indicating a thickness of the DAE blend film of ~2.6 nm (Figure S2d). Figures 2a and 2b display the evolution of forward gate sweeping transfer characteristics of the FET devices under different light irradiation, in both linear and logarithmic scale. All the devices on Si/SiO_2 substrate are measured at drain-source voltage V_{ds} = 2 V and gate voltage V_g ranging from -90 to 90 V. The initial WSe_2 device without DAE molecules features a typical ambipolar behavior with pristine hole mobility of 71.5 $cm^2 V^{-1} s^{-1}$ and electron mobility of 21.6 $cm^2 V^{-1} s^{-1}$. Once the DAE blend is physisorbed on the WSe_2 surface, the threshold voltages for both holes and electrons move towards negative directions, whereas the hole mobility decreases to 49.2 $cm^2 V^{-1} s^{-1}$ and the electron mobility increases to 25.1 $cm^2 V^{-1} s^{-1}$. These phenomena indicate that the DAE blends, with both photochromes in their open state, induce an n-type doping effect on WSe_2. As a result of UV irradiation, a decrease of mobility can be observed for both holes (μ_{h^+} = 2.1 $cm^2 V^{-1} s^{-1}$) and electrons (μ_{e^-} = 16.9 $cm^2 V^{-1} s^{-1}$), accompanied with a downshift of threshold voltage for holes ΔV_{th-h^+}= -4.8 V and a upshift for electrons ΔV_{th-e^-} = 19.1 V. Therefore, the closed-form of DAE in the blend simultaneously deplete electrons and holes from WSe_2 with $\Delta n_{h^+} = 3.8 \times 10^{11}$ cm^{-2} and $\Delta n_{e^-} = 1.5 \times 10^{12}$ cm^{-2}, indicating a n-type doping effect on hole transport while p-type doping effect on electron transport. The modulation process was proven to be reversible by successive vis light irradiation. In this process, switching the DAE molecules back to the open-form fully restores the initial electrical performance. An additional backward gate sweeping measurement is illustrated in Figure S3, which shows the same trend as the forward sweeping, proving that the hysteresis has no influence on the carrier transport modulation. To eliminate the contribution from WSe_2, transfer curves of the reference device with pristine WSe_2 were also measured, which shows no variation under dark and after UV/vis illumination

(Figure S4a). In order to prove the reproducibility of such current modulation, we investigated 8 devices each based on WSe_2 flakes with similar thicknesses. The devices show stable current modulation efficiencies under the same experimental conditions, with hole current modulation efficiencies varying from 95% to 98% and electron current modulation efficiencies varying from 48% to 53%. Such minor differences can be attributed to the interface quality between WSe_2 and DAE blends.

Due to the full recovery of all the electrical characteristics of the FET device after subsequent vis light irradiation, more illumination cycles can be launched to test the stability of such photo-modulation of the current. In Figure 2c we plot the normalized drain current I_{ds} for both holes and electrons taken from the transfer curves obtained during the 10 measured cycles (I_0 is the current value measured in step 0, which corresponds to the current initially after molecular deposition. Figure S5 plots the detailed transfer curves.). The hole current is collected at V_g = -90 V and the electron current is collected at V_g = 90 V. The current modulation is as high as 97% for holes and 52% for electrons, showing a more efficient trapping for holes than for electrons. Note that different mix weight ratios of the two DAE molecules are tested (from 1:10 to 10:1), but the current modulation efficiency remains unchanged. Therefore we attribute the observed difference of modulation efficiency to the fact that the energy difference between the VBM of WSe_2 and the HOMO of DAE_2c (0.4 eV) is larger than that between the CBM of WSe_2 and the LUMO of DAE_1c (0.2 eV), thus triggering the a more efficient trapping of holes when compared to electrons. This result is also in accordance with our previous established models when DAE molecules are blended with different organic semiconductors.[37] The absence of degradation after 10 illumination cycles shows that our devices possess reasonable stability and robustness.

Figure S6 displays the output measurement of the FET based on DAE blend decorated WSe_2. The curves present a linear and symmetric correlation between the drain current I_{ds} under different drain biases V_{ds}, demonstrating a low contact resistance of WSe_2 with Au electrodes

regardless of the photo-isomeric state adopted by the DAE molecules. The current also shows similar modulation tendency as the results obtained from transfer curves, *i.e.* under the same applied gate voltage: the current for DAE_c modified WSe_2 exhibits a downshift when compared with DAE_o modified WSe_2.

To better illustrate the photo-modulation of the DAE blend-WSe_2 FET device, Figure 2d displays the dynamic behavior of drain current for holes at -90 V gate voltage during 20 illumination cycles and Figure S7c shows one single cycle (each cycle includes four steps, *i.e.* 5 s UV, 30 s dark, 40 s vis, 30 s dark). The red boxed region is the period when UV is on and the blue boxed region indicates when vis is on. The same measurement performed for electron current at 90 V gate voltage is shown in Figures S6d and S6e. Note that the curves are corrected for gate bias stress effect to single out the sole contribution of molecular switching (original curves and gate bias curves are provided in Figures S7a and S7b).[38] By comparing the curves obtained, we find that the electron and hole current show the same modulation tendency under light irradiation. When the light is switched on and off, the current displays a sudden increase or drop behavior, which is described as the photocurrent triggered by the generation and relaxation of electron-hole pairs.[39] During the illumination of UV light, the conversion of open to closed isomers is a time-resolved process, which leads to a gradual depletion of electrons and holes from the WSe_2 channel, resulting in a gradual decrease of the current. Conversely, under subsequent vis light illumination the current increases gradually owing to the relaxation of molecules from closed to open isomers. At the end of each cycle, the current recovers to the original value confirming that all the charge carriers are transferred back to WSe_2. In Figure 2d and S7d, we observe that after over 20 illumination cycles the modulation shows no noticeable fatigue, indicating the excellent endurability of our device. The control experiment on pristine WSe_2 device is also performed under the same UV/vis illumination conditions. As displayed in Figure S4b and S4c, the device exhibits only photoresponse upon light exposure whereas no significant modulation is observed. Moreover, the photocurrent in pristine WSe_2 is one order

of magnitude smaller than that decorated by the DAEs. Therefore, the photo-modulation of charge transport in WSe_2 can be ascribed to the molecular photoswitching behavior.

The drain current level for both holes and electrons are proportional to the population ratio between DAE_o and DAE_c molecules, which can be controlled by the light illumination dose. In **Figure 3a and 3d** we portray the multilevel current for holes and electrons respectively, which are obtained by illuminating the device at different fixed times at a well-defined areal power density. We start from Level 1, at which the current state is the result of both two DAE molecules in open forms. Later, Level 2 to Level 5 are reached after UV irradiation for 10 s, 20 s, 40 s, and 80 s, and Level 5 is the current state when all the molecules are in closed forms. By subsequent vis illumination, the current value can be restored to Level 1. Such illumination cycle is repeated for 5 times and the values obtained for each level are quite stable. Their standard deviations are calculated to be below 1.5% of the total current difference (I_{ds}_o – I_{ds}_c), thus demonstrating that the device can attain multiple current levels precisely by remote light control (detailed values for each level are provided in **Table S1** and **S2**). To further investigate the number of levels our device can reach, we perform the I_{ds}-time test by exposing the device to a periodic UV light irradiation at intervals of 20 s (60 s – 540 s: 0.5 s per 20 s; 540 s – 860 s, 1 s per 20 s; 860 s – 1020 s: 2 s per 20 s, 1020 s – 1180 s: 4 s per 20 s; 1180 s – 1340 s: 8 s per 20 s). Figure 3b and 3e display the results: the current follows a progressive decrease after each light dose and the value holds stable at that level, representing a continuous depletion of charge carriers in WSe_2. It was possible to attain 64 current levels for both holes and electrons with clear current changes between adjacent levels. Figures S8 and S9 provide the detailed plots, justifying the validity of each current level. Therefore, a 128-level-device with a data storage capacity of 7 bit and a high accuracy readout was successfully built.

The unique thermal bistability of the DAE molecules can be expected to endow to the devices a good retention capacity. By keeping the device in the dark, we independently measure its hole and electron current after different storage times. The results are plotted in Figure S10.

They reveal a highly reliable retention characteristic with the current remaining stable for both isomer states over 20 days. For each current level, the standard deviation is below 1.5% of the total current difference (**Table S3**), demonstrating a remarkable retention capacity, which is essential for a commercial non-volatile memory.

To further elucidate the contribution of two DAE molecules individually, we perform the electrical measurement on WSe_2 devices with only DAE_1 or DAE_2. As displayed in Figure S10, the device with DAE_1 presents only electron transport modulation under illumination conditions and hole current has no obvious variation. Comparatively, the device with DAE_2 can only modulate hole transport. Their current modulation efficiencies quantitatively match the results obtained in the DAE blend decorated device (~52% for DAE_1 and ~97% for DAE_2). These phenomena clarify that the two molecules work separately and have no disturbance between each other.

In order to demonstrate the general adaptability of our multilevel device into future flexible/wearable memories, the as-fabricated WSe_2 FET on Si/SiO_2 substrate is transferred onto a flexible PET substrate with indium tin oxide (ITO) serving as back-gate electrode and 80 nm cross-linked poly(4-vinylphenol) (CL-PVP) as dielectric material. The detailed transfer process is illustrated in Figure S12. **Figure 4a** shows a photograph of a typical flexible and transparent device and the inset displays its corresponding schematic structure and optical microscopic images. The device exhibits a hole mobility of 35.5 $cm^2\ V^{-1}s^{-1}$ and electron mobility of 43.3 $cm^2V^{-1}s^{-1}$, which is comparable to values obtained on rigid Si/SiO_2 substrates, suggesting that the transfer process does not significantly diminish the device's electrical performance. The transfer characteristics evolution after molecular deposition and light irradiation is displayed in Figure 4b. The device retains its photo-modulation ability with a hole current modulation of 96% and electron current modulation of 49%, being slightly lower than the obtained values on Si/SiO_2 substrate. We attribute this to the difference of interface quality between the substrates. The dynamic electron current variation at 90 V gate voltage during 6

illumination cycles is also investigated, revealing a similar trend as on Si/SiO_2 substrate: UV light yields a sizable drop of the current while vis light triggers the current to return to the original value. Furthermore, a series of bending tests are performed to investigate the influence of bending cycles on the current modulation efficiency. Each cycle consists of 5 s of bending at a bending radius of 8 mm, followed by 20 s of resting time. After specific bending cycles, the device is exposed to one illumination cycle with alternate UV/vis irradiation and the corresponding transfer curves are collected. As displayed in Figure 4d, the effect of bending cycles on the current modulation efficiency is found to be negligible. Over 100 bending cycles are monitored, both hole and electron currents can virtually preserve their modulation efficiency, suggesting a good mechanical stability of our device on the flexible substrate (detailed transfer curves collected are provided in Figure S13).

In conclusion, we have successfully fabricated WSe_2-based optically switchable FET by interfacing such 2DM with a blend of two photochromic DAE molecules acting as light-sensitive components. Upon light illumination, the device can modulate hole and electron transport simultaneously for at least 20 cycles with a good endurance. The electrical characterizations provide unambiguous evidence that suitably designed DAE molecules with phototunable frontier molecular orbital energy levels can systematically tune the charge transport of the target 2DM. We clearly demonstrate the feasibility and generality of our approach to optically control the transport of electrons, or holes, or both charge carriers, depending on the nature of the target 2DM, thus it offers intriguing perspectives for optically switchable ambipolar FETs based on photochromic molecules/2DMs hybrid systems. Noteworthy, our device exhibits a combination of 128 distinct current levels with a high accuracy readout and over 20 days of retention time, which is of paramount importance for future applications as multilevel non-volatile memories. Our devices are also compatible to work on flexible PET substrates as their light responsive properties are successfully preserved, and thus offer a versatile platform for applications in flexible and transparent electronics.

Experimental Section

Experimental details are available in the Supporting Information.

Supporting Information

Supporting Information is available from the Wiley Online Library or from the author.

Acknowledgements

We acknowledge funding from the European Commission through the ERC projects SUPRA2DMAT (GA-833707) and Light4Function (GA-308117), the Graphene Flagship Core 2 project (GA-785219), the Marie Sklodowska-Curie projects ITN project iSwitch (GA-642196), the M-ERA.NET project MODIGLIANI, the Agence Nationale de la Recherche through the Labex projects CSC (ANR-10-LABX-0026 CSC) and NIE (ANR-11-LABX-0058 NIE) within the Investissement d'Avenir program (ANR-10-120 IDEX-0002-02), the International Center for Frontier Research in Chemistry (icFRC), the German Research Foundation (DFG via SFB 658 and SFB 951) as well as the Chinese Scholarship Council.

Received: ((will be filled in by the editorial staff))
Revised: ((will be filled in by the editorial staff))
Published online: ((will be filled in by the editorial staff))

References

[1] F. Bonaccorso, Z. Sun, T. Hasan, A. C. Ferrari, *Nat. Photonics* **2010**, *4*, 611.

[2] Q. H. Wang, K. Kalantar-Zadeh, A. Kis, J. N. Coleman, M. S. Strano, *Nat. Nanotechnol.* **2012**, *7*, 699.

[3] G. Fiori, F. Bonaccorso, G. Iannaccone, T. Palacios, D. Neumaier, A. Seabaugh, S. K. Banerjee, L. Colombo, *Nat. Nanotechnol.* **2014**, *9*, 768.

[4] F. Xia, H. Wang, D. Xiao, M. Dubey, A. Ramasubramaniam, *Nat. Photonics* **2014**, *8*, 899.

[5] S. Mao, J. Chang, H. Pu, G. Lu, Q. He, H. Zhang, J. Chen, *Chem. Soc. Rev.* **2017**, *46*, 6872.

[6] C. Anichini, W. Czepa, D. Pakulski, A. Aliprandi, A. Ciesielski, P. Samorì, *Chem. Soc. Rev.* **2018**, *47*, 4860.

[7] S. Das, R. Gulotty, A. V. Sumant, A. Roelofs, *Nano Lett.* **2014**, *14*, 2861.

[8] N. Petrone, T. Chari, I. Meric, L. Wang, K. L. Shepard, J. Hone, *ACS nano* **2015**, *9*, 8953.

[9] D. Akinwande, N. Petrone, J. Hone, *Nat. Commun.* **2014**, *5*, 5678.

[10] P. Samorì, V. Palermo, X. Feng, *Adv. Mater.* **2016**, *28*, 6027.

[11] V. P. Pham, G. Y. Yeom, *Adv. Mater.* **2016**, *28*, 9024.

[12] K. Haynes, R. Murray, Z. Weinrich, X. Zhao, D. Chiappe, S. Sutar, I. Radu, C. Hatem, S. S. Perry, K. S. Jones, *Appl. Phys. Lett.* **2017**, *110*, 262102.

[13] S. Bae, N. Sugiyama, T. Matsuo, H. Raebiger, K.-i. Shudo, K. Ohno, *Phys. Rev. Appl.* **2017**, *7*, 024001.

[14] M. E. Itkis, X. Chi, A. W. Cordes, R. C. Haddon, *Science* **2002**, *296*, 1443.

[15] C. Simão, M. Mas-Torrent, N. Crivillers, V. Lloveras, J. M. Artés, P. Gorostiza, J. Veciana, C. Rovira, *Nat. Chem.* **2011**, *3*, 359.

[16] Z. Liu, H. I. Wang, A. Narita, Q. Chen, Z. Mics, D. Turchinovich, M. Kläui, M. Bonn, K. Müllen, *J. Am. Chem. Soc.* **2017**, *139*, 9443.

[17] S. Bertolazzi, M. Gobbi, Y. Zhao, C. Backes, P. Samorì, *Chem. Soc. Rev.* **2018**, *47*, 6845.

[18] M. Gobbi, E. Orgiu, P. Samorì, *Adv. Mater.* **2018**, *30*, 1706103.

[19] L. Wang, Q. Li, *Chem. Soc. Rev.* **2018**, *47*, 1044.

[20] Y. Zhao, S. Ippolito, P. Samorì, *Adv. Opt. Mater.* **2019**, 1900286.

[21] X. Zhang, L. Hou, P. Samorì, *Nat. Commun.* **2016**, *7*, 11118.

[22] M. Gobbi, S. Bonacchi, J. X. Lian, A. Vercouter, S. Bertolazzi, B. Zyska, M. Timpel, R. Tatti, Y. Olivier, S. Hecht, M. V. Nardi, D. Beljonne, E. Orgiu, P. Samorì, *Nat. Commun.* **2018**, *9*, 2661.

[23] A.-R. Jang, E. K. Jeon, D. Kang, G. Kim, B.-S. Kim, D. J. Kang, H. S. Shin, *ACS nano* **2012**, *6*, 9207.

[24] Y. Zhao, S. Bertolazzi, P. Samorì, *ACS nano* **2019**, *13*, 4814.

[25] M. Kim, N. S. Safron, C. Huang, M. S. Arnold, P. Gopalan, *Nano Lett.* **2012**, *12*, 182.

[26] H. Qiu, Y. Zhao, Z. Liu, M. Herder, S. Hecht, P. Samorì, *Adv. Mater.* **2019**, *31*, 1903402.

[27] P. R. Pudasaini, A. Oyedele, C. Zhang, M. G. Stanford, N. Cross, A. T. Wong, A. N. Hoffman, K. Xiao, G. Duscher, D. G. Mandrus, T. Z. Ward, P. D. Rack, *Nano Res.* **2018**, *11*, 722.

[28] M. Irie, T. Fukaminato, K. Matsuda, S. Kobatake, *Chem. Rev.* **2014**, *114*, 12174.

[29] T. Tsujioka, H. Kondo, *Appl. Phys. Lett.* **2003**, *83*, 937.

[30] M. Min, S. Seo, S. M. Lee, H. Lee, *Adv. Mater.* **2013**, *25*, 7045.

[31] L. A. Frolova, A. A. Rezvanova, B. S. Lukyanov, N. A. Sanina, P. A. Troshin, S. M. Aldoshin, *J. Mater. Chem. C* **2015**, *3*, 11675.

[32] S. Bertolazzi, P. Bondavalli, S. Roche, T. San, S.-Y. Choi, L. Colombo, F. Bonaccorso, P. Samorì, *Adv. Mater.* **2019**, *31*, 1806663.

[33] T. Leydecker, M. Herder, E. Pavlica, G. Bratina, S. Hecht, E. Orgiu, P. Samorì, *Nat. Nanotechnol.* **2016**, *11*, 769.

[34] K. Börjesson, M. Herder, L. Grubert, D. Duong, A. Salleo, S. Hecht, E. Orgiu, P. Samorì, *J. Mater. Chem. C* **2015**, *3*, 4156.

[35] M. Herder, B. M. Schmidt, L. Grubert, M. Pätzel, J. Schwarz, S. Hecht, *J. Am. Chem. Soc.* **2015**, *137*, 2738.

[36] Y. Guo, J. Robertson, *Appl. Phys. Lett.* **2016**, *108*, 233104.

[37] E. Orgiu, N. Crivillers, M. Herder, L. Grubert, M. Pätzel, J. Frisch, E. Pavlica, D. T. Duong, G. Bratina, A. Salleo, N. Koch, S. Hecht, P. Samorì, *Nat. Chem.* **2012**, *4*, 675.

[38] K. Cho, W. Park, J. Park, H. Jeong, J. Jang, T.-Y. Kim, W.-K. Hong, S. Hong, T. Lee, *ACS nano* **2013**, *7*, 7751.

[39] Y.-C. Wu, C.-H. Liu, S.-Y. Chen, F.-Y. Shih, P.-H. Ho, C.-W. Chen, C.-T. Liang, W.-H. Wang, *Sci. Rep.* **2015**, *5*, 11472.

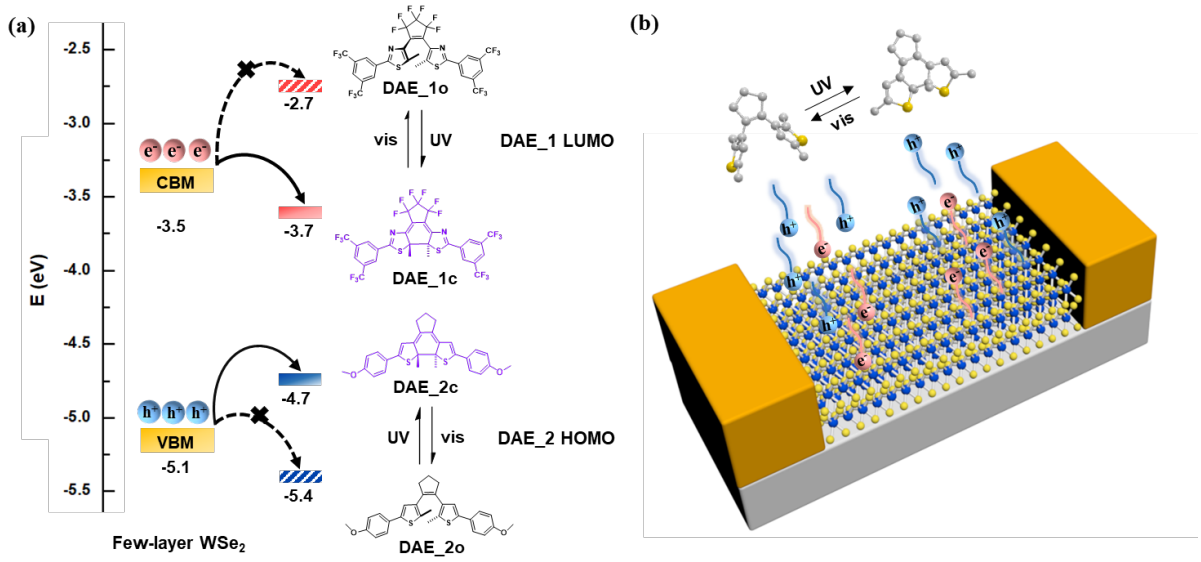

Figure 1: Energy level diagram, molecular and device structure. (a) Chemical structures of DAE_1 and DAE_2, as both open and closed isomers. Energy level diagram of electron transport between WSe_2/DAE_1 and hole transport between WSe_2/DAE_2. Energy level values for WSe_2 are calculated in the screened exchange functional, and the values for DAEs are measured by cyclic voltammetry. (b) Schematic illustration of the FET device architechture based on WSe_2/DAE blend on Si/SiO_2 substrate.

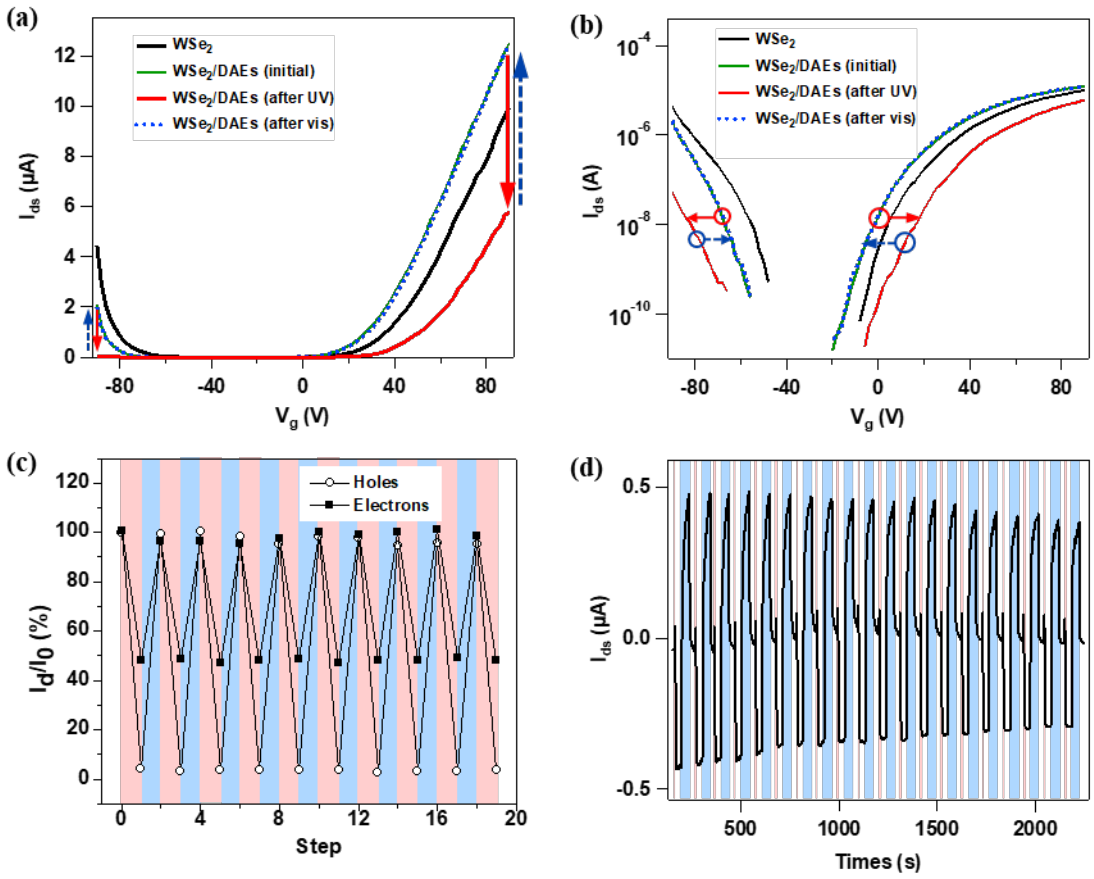

Figure 2. Electrical characterization of WSe_2/DAE blend FET device. (a) and (b) Transfer evolution of pristine WSe_2, WSe_2/DAE blend as prepared and after UV/vis irradiation in (a) linear and (b) logarithmic scale. (c) Drain current I_{ds} modulation as both open and closed isomers over 10 illumination cycles with alternative UV (red shaded areas) and vis (blue shaded areas) light. All current values are normalized to the initial value obtained from the as prepared WSe_2/DAE blend. The connecting lines are used as guides to the eye. (d) Dynamic I_{ds}-time measurement (corrected for bias stress effect) under alternative dark and UV/vis illumination conditions at V_g = -90 V, V_{ds} = 2 V for WSe_2/DAE blend duing 20 cycles.

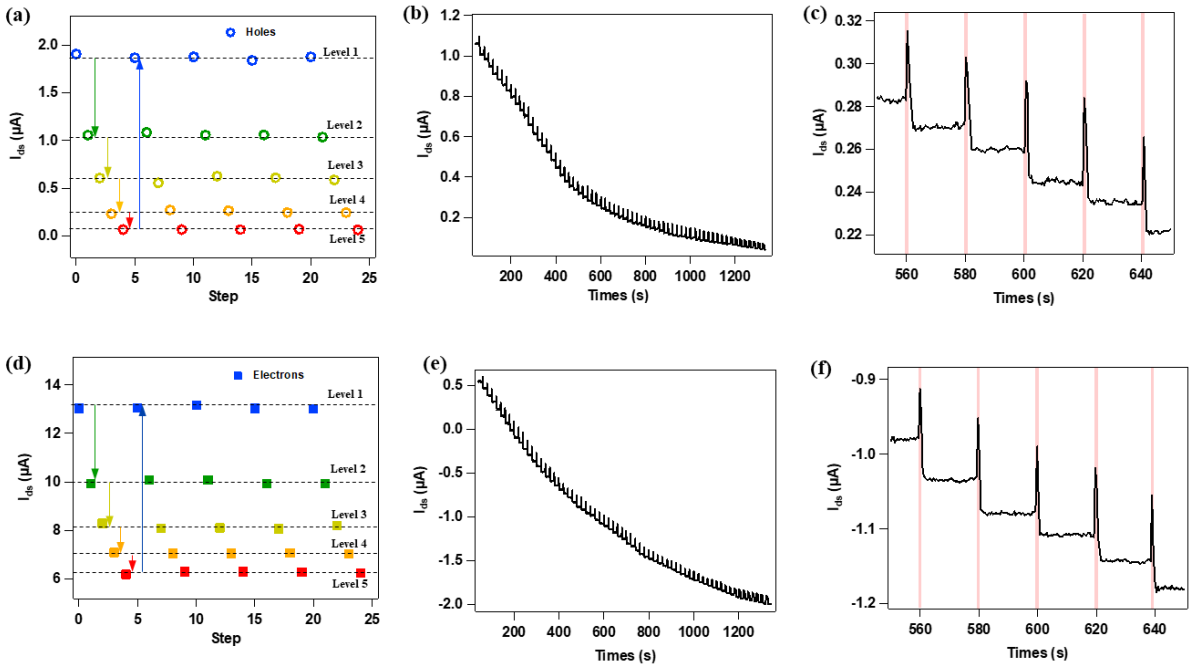

Figure 3. Multilevel characterization of WSe_2/DAE blend FET device. (a) 5 distinct current levels over 5 illumination cycles for holes recorded at V_g = -90 V. The levels are obtained by illuminating the device for different fixed times. (b) and (c) Dynamic hole current I_{ds}-time curves (corrected for bias stress) under periodic UV irradiation per 20 s, (b) 64 levels are achieved in total, (c) an enlargement of 5 levels. (d) to (f) Same measurements for electrons recorded at V_g = 90 V.

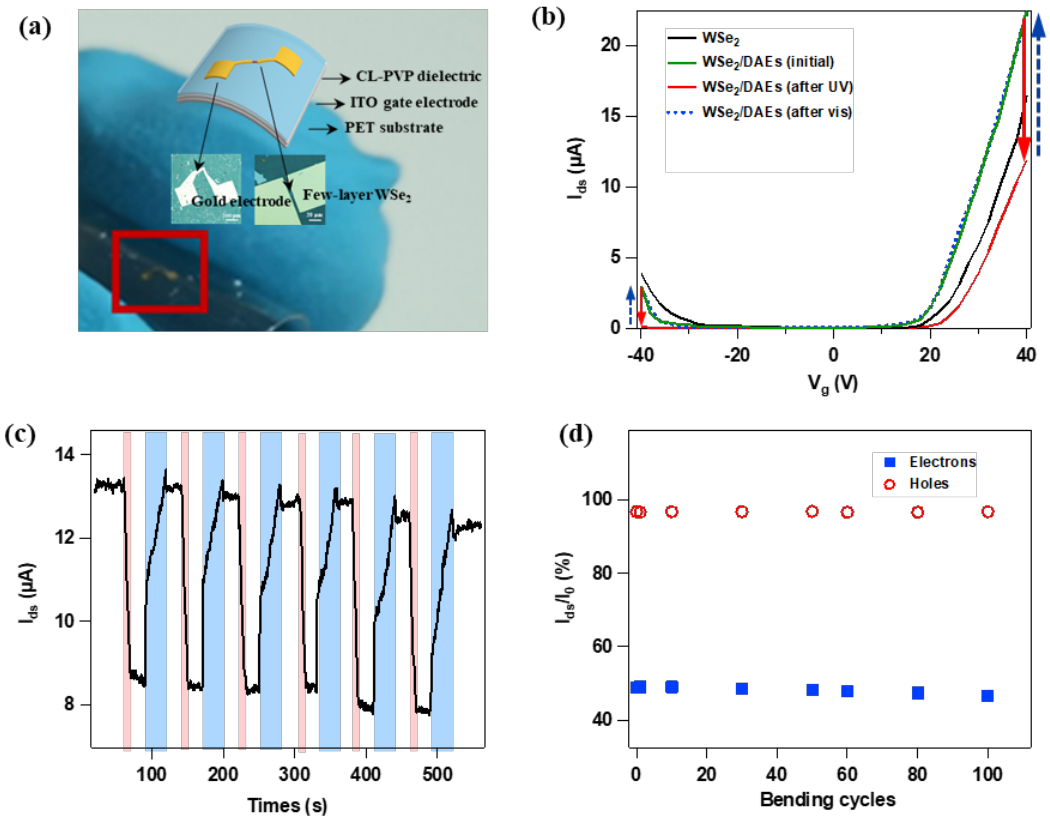

Figure 4. Structure and electrical characterization of WSe_2/DAE blend FET device on flexible substrate. (a) Photograph of a typical flexible and transparent device on PET substrate. Inset: Schematic (up) and corresponding optical microscopic images (down) of FET device. (b) Transfer evolution of pristine WSe_2, WSe_2/DAE blend FET as prepared and after UV/vis irradiation. (c) Dynamic I_{ds}-time measurement under alternative dark and UV/vis illumination conditions during 6 cycles at $V_g = 90$ V, $V_{ds} = 2$ V for WSe_2/DAE blend FET. (d) Drain current modulation efficiency as a function of bending cycles.